PAPER

Spectrum and energy levels of quadruply-ionized molybdenum (Mo V)

View the article online for updates and enhancements.

Spectrum and energy levels of quadruply-ionized molybdenum (Mo V)

Joseph Reader and Ahmad Tauheed[1]

National Institute of Standards and Technology, Gaithersburg, MD 20899-8422, USA

E-mail: joseph.reader@nist.gov

Abstract

The spectrum of quadruply-ionized molybdenum Mo V was observed from 200 to 4700 Å with sliding spark discharges on 10.7 m normal- and grazing-incidence spectrographs. The existing analyses of this spectrum (Tauheed *et al* 1985 *Phys. Scr.* **31** 369; Cabeza *et al* 1986 *Phys. Scr.* **34** 223) were extended to include the $5s^2$, $5p^2$, $5s5d$, $5s6s$, $4d5f$, and $4d5g$ configurations as well as the missing $^3H_6$ level of $4d4f$ and about 75 levels of the core-excited configuration $4p^54d^3$. The values of the $4d5d$ $^1S_0$, $5s5p$ $^1P_1$, and $4d6p$ $^3P_0$ levels were revised. There are now about 900 lines classified as transitions between 66 even parity and 191 odd parity energy levels. Of these, about 600 lines and 130 levels are new. From the optimized energy level values, Ritz-type wavelengths were determined for about 380 lines, with uncertainties varying from 0.0003 to 0.002 Å. The observed configurations were theoretically interpreted by means of Hartree–Fock calculations and least-squares fits of the energy parameters to the observed levels. The fitted parameters were used to calculate oscillator strengths for all classified lines. A few unclassified lines and undesignated levels are also given. An improved value for the ionization energy was obtained by combining the observed energy of the $4d5g$ configuration with an *ab initio* calculation of its term value. The adopted value is $438\,900 \pm 150$ cm^{-1} (54.417 ± 0.019 eV).

S Online supplementary data available from stacks.iop.org/JPB/48/144001/mmedia

Keywords: wavelengths, energy levels, transition probabilities, ionization energy, vacuum ultraviolet

1. Introduction

We present a comprehensive updating and expansion of the spectrum and energy levels of quadruply-ionized molybdenum, Mo V. These results will be of interest for diagnoses of plasmas that contain Mo as a constituent. Walls of fusion reactors often contain alloys of Mo, and ions of Mo will be present in the plasma due to sputtering from the walls. These results will also be of interest for extension of the structure of strontium-like ions to higher stages of ionization. In particular, our location of the core-excited configuration $4p^54d^3$ will be of direct interest for further understanding of the structure of the Sr-like ion Sn XIII [1], expected to be important for development of radiation sources of

nanolithography. The theory of the $4p^54d^3$–$4p^64d4f$ configuration interaction (CI) has been studied recently by Kučas *et al* [2].

MoV is a member of the Sr isoelectronic sequence. The ground configuration is $4p^64d^2$. Excited configurations are mainly of the type $4dnl$ or $5snl$. The first assignments in this spectrum were given by Trawick [3]. He classified 90 lines connecting 36 energy levels of the (partially complete) $4d^2$, $4d5s$, $4d5p$, $4d5d$, and $4d4f$ configurations. Trawick's levels are summarized in the atomic energy levels compilation [4]. In 1985 Tauheed *et al* [5] extended the level system to a number of higher configurations. These were only partially confirmed by the 1986 analysis of Cabeza *et al* [6], who classified about 400 lines representing transitions between the nearly complete $4d^2$, $4d5s$, $4d5p$, $4d5d$, $4d4f$, $5s5p$, $4d6s$, and $4d6p$ configurations. Much of the data for this analysis [6] consisted of spectrograms supplied by Kaufman of the National Institute of Standards and Technology (NIST) to the

[1] Permanent address: Physics Department, Aligarh Muslim University, Aligarh-202002, India.

Instituto de Optica in Spain and of wavelengths for Mo V measured by Reader of NIST, supplied to Meijer of the Zeeman Laboratorium in The Netherlands in 1979.

The present work was begun to locate the 4d5g configuration in Mo V. In both Zr III [7] and Nb IV [8], this configuration was found to make strong transitions to 4d4f, and since spectra of Mo were already available in our laboratory, it was likely that extension of the 4d4f–4d5g transitions to Mo V would be relatively straightforward. Although this goal was accomplished, it proved to be less than straightforward. We also had the goal of extending the analysis to the core-excited configurations $4p^5 4d^3$ and $4p^5 4d^2 5s$. Since we expected these configurations to make strong transitions to the ground configuration $4p^6 4d^2$ in the 200–400 Å region, and since we observed strong lines of Mo V in this region, we thought that this would also be relatively straightforward. In fact, although many of these highly-excited levels could be established, due to complex CIs between these levels and levels of the two-electron system $4p^6 4dnf$, unambiguous assignment of the levels proved difficult. All of the core-excited levels that we observed were of the type $4p^5 4d^3$. As the $4p^5 4d^2 5s$ configuration lies very high, with nearly half of its levels falling above the ionization limit, we were not able to reliably establish any of its levels.

We have now found new levels that replace the 5s5p $^1P_1$, 4d6p $^3P_0$, and 4d5d $^1S_0$ levels of Cabeza *et al* [6]. Except for these three levels, we confirmed the analysis of Cabeza *et al* [6], and we consider this as the starting point for our present knowledge of this spectrum. Additionally, we report 52 new energy levels of the $5s^2$, $5p^2$, 5s5d, 5s6s, 4d5f, and 4d5g configurations, which are practically complete, as well as about 75 levels of $4p^5 4d^3$. The missing $^3H_6$ level of the already known 4d4f configuration was also located. We determined an improved ionization energy for Mo V, based on the observed position of the 4d5g configuration.

2. Experiment

The light source was a sliding spark discharge between solid Mo electrodes across a quartz spacer. The spark was operated as described by Reader *et al* [9]. The spectra were photographed in the 200–4700 Å region with the NIST 10.7 m grazing-incidence and 10.7 m normal-incidence vacuum spectrographs. These spectrographs both have gratings with 1200 lines/mm. The plate factor for the grazing-incidence spectrograph at 340 Å was 0.25 Å mm^{-1}. The plate factor for the normal-incidence spectrograph was 0.78 Å mm^{-1}. This was nearly constant over our range of observation. Complete experimental details including calibration procedures and reference spectra are given in the reports on Mo VI by Reader [10] and Mo VII by Reader and Feldman [11].

Peak currents in the spark varied from 300 to 4000 A. Ionization stages were determined by comparing the intensities of the lines at the various peak currents. Spectra of Mo V were relatively enhanced at a peak current of 500 A. A portion of the spectrum is shown in figure 1. The good separation of ionization stages is evident. The intensities of
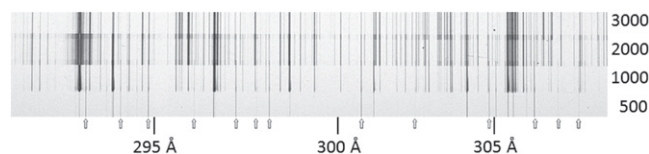

Figure 1. Sliding spark spectrum of Mo in 290–310 Å region. Peak currents in the spark in A are indicated at the right. Prominent lines of Mo V are indicated with arrows.

the Mo V lines are nearly identical at peak currents of 500 and 1000 A. Lines of Mo VI are greatly enhanced at 1000 A and remain nearly constant at 2000 and 3000 A. Lines of Mo VII are enhanced at 2000 A.

The wavelengths, intensities, wave numbers, and classifications of the observed lines of Mo V are given in table 1. (The complete table 1 is given in the supplementary materials.) The uncertainty of the wavelengths shorter than 2300 Å is estimated as ±0.005 Å; for wavelengths longer than 2300 Å the uncertainty is estimated as ±0.010 Å. All uncertainties are estimated at the level of one-standard deviation. In order to provide a unified description of this spectrum, we have included in table 1 the lines identified by Cabeza *et al* [6]. All wavelengths are from our present measurements. We also include in table 1 several lines in the short wavelength region that clearly belong to Mo V, but remain unclassified. They likely represent transitions to the ground configuration $4p^6 4d^2$ from $4p^5 4d^2 5s$.

The intensities in table 1 are visual estimates of plate blackening. The values range from 1 to 900 000. The system that we use to obtain this extensive scale of intensities is described in detail in our paper on Nb IV [8]. For the present set, no attempt was made to account for variation in spectrograph or plate emulsion response. The strongest lines of the spectrum comprise a group of 4d5s–4d5p transitions lying in the region 1500–2000 Å.

The even parity energy levels are given in table 2. The odd parity levels are given in table 3. The level values were optimized with the computer program ELCALC [12], an iterative procedure in which the observed wave numbers are weighted according to the inverse square of their uncertainties. The uncertainties of the level values given by this procedure are also listed. The levels are designated in either LS or *jl* coupling. They are also given shorthand designations that are used for the classifications of the spectral lines. The shorthand designations are explained in the footnotes to table 2.

In comparing our present wavelengths with those of Cabeza *et al* [6], it is seen that many of the wavelengths are in very good agreement. Quite a few are identical. This is a consequence of their use of our wavelength material for much of their analysis of [6]. Concerning their observed lines, we note that: (1) 358.420 Å is due to a higher stage of ionization; (2) 364.349 Å is due to a higher stage, probably Mo VIII; (3) 374.163 Å is actually O III at 374.165 Å, hence the poor fit to their energy levels; we have taken our present wavelength and intensity from an exposure that was free from interference from O III; (4) 422.135 Å is second order of a higher stage

Table 1. Observed spectral lines of Mo V. Wavelengths (Å) are in vacuum. Newly observed lines are noted with N. Complete table is given in supplementary materials.

λ	Intensity		σ(cm^{-1})	Even level[a]	Odd level[a]	λ(Ritz)	Uncertainty	gA(s^{-1})	log(gf)
248.019	70	N	403 195						
248.230	40	N	402 852	d211	u03				
248.516	20	N	402 389						
248.708	75	N	402 078						
248.759	15	N	401 996	d212	9f12			5.64E+10	−0.28
4638.973	50	N	21556.495	6s22	6p13			3.21E+07	−0.99
4688.586	30	N	21328.392	6s13	6p22			3.41E+07	−0.95

[a] Level codes are explained in table 2.

Symbols: A, masked by O IV—Ritz value; B, masked by Si IV—Ritz value; dc, doubly classified; p, perturbed by close line; u, unresolved from close line; h, hazy; s, shaded to shorter wavelength.

line at 211.068 Å, probably Mo VIII; (5) 434.786 Å is second order of a Mo VI line at 217.394 [10]; (6) 434.876 Å is due to Mo VII at 434.881 Å [11]; (7) 555.259 Å is due to O IV at 555.261 Å.

3. Ritz wavelengths

In table 1 we list wavelengths determined from the optimized level values, or Ritz values. The uncertainties of the Ritz wavelengths correspond to the square root of the sum of the squares of the uncertainties of the combining levels. The Ritz wavelengths have uncertainties varying from ±0.0003 to ±0.0020 Å. They should be useful for astrophysical line identifications and for general wavelength calibration in the vacuum ultraviolet, especially where sliding spark discharges are used.

4. Spectrum analysis

Figure 2 shows a schematic overview of the configurations and transition groups that we observed for Mo V. Newly observed configurations are noted with a #. Some of these configurations have been only partially observed. Interpretation of the spectrum was guided by calculations of the level structures and transition probabilities carried out with the Hartree–Fock code of Cowan [13]. Further guidance was given by construction of two-dimensional transition arrays with the computer spreadsheet method described by Reader [14].

4.1. $4d^2 + 4d5s + 5s^2$ levels

Except for $5s^2$ $^1S_0$, all levels of this group were given by Cabeza et al [6]. To find $5s^2$ $^1S_0$ in Mo V, we first compared its observed position in Zr III and Nb IV with the position predicted with the Hartree–Fock calculations. Using this comparison as a guide, we located this level in Mo V at 199 050.88 cm^{-1}. The $5s^2$ $^1S_0$ level makes a strong transition to $5s5p$ $^1P_1$ at 1316.250 Å. The level position is confirmed by additional transitions to levels of 4d6p (1155.156 and 1279.790 Å) and 4d4f (1757.764 Å). A recent ab initio

calculation of this level by Pan and Beck [15] predicts $5s^2$ $^1S_0$ to lie at 196 717 cm^{-1}. The agreement here is not as good as was obtained by these authors [16] for Zr III, where the calculated value of 48 712 cm^{-1} compared to the experimental value [7] of 48 507 cm^{-1}, and for Nb IV, where the calculated value of 116 826 cm^{-1} compared to the experimental value [8] of 116 921.51 cm^{-1}.

The $4d^2 + 4d5s + 5s^2$ levels are plotted in figure 3. The diagonal lines in these level diagrams connect the various terms, either in LS- or jl-coupling.

4.2. 4d5p + 5s5p levels

These are the lowest levels of odd parity, and their combinations with the $4d^2 + 4d5s + 5s^2$ levels constitute the strongest lines of the spectrum. All of these levels were given by Cabeza et al [6]. They are plotted in figure 4.

In Cabeza et al [6] the $5s5p$ $^1P_1$ level, 273 199.0 cm^{-1}, was determined by four lines: 380.227, 381.640, 384.940, and 575.316 Å, which did not fit well together. Their value for this level was based almost exclusively on the line at 575.316 Å, $4d5s$ $^1D_2$–$5s5p$ $^1P_1$, which is the only strong transition expected for the $5s5p$ $^1P_1$ level. We find that the lines 380.227, 381.640, and 384.940 Å do not belong to Mo V. The line at 575.316 Å did not appear in our spectra. Our new value of 275 024.26 cm^{-1} is based mainly on the $4d5s$ $^1D_2$–$5s5p$ $^1P_1$ transition at 569.335 Å. This is supported by observation of the $4d5s$ $^3D_2$–$5s5p$ $^1P_1$ transition at 549.715 Å.

In Cabeza et al [6] the level at 246 800.0 cm^{-1} was identified as $5s5p$ $^3P_1$ and the level at 247 933.0 cm^{-1} as $4d4f$ $^3D_1$. Based on our present observed intensities and calculations, we find that the identifications of these levels should be interchanged. They are given with interchanged designations in table 3.

4.3. 4d5d + 4d6s levels

Although all of these were given in [6], $4d5d$ $^1S_0$ was given as an uncertain level at 251 093.7 cm^{-1}. We have now located this level at 251 017.96 cm^{-1} by means of several transitions to 4d5p, 4d4f, and 4d5f. This position agrees well with our least-squares fits of the energy parameters to the observed levels, described below.

Table 2. Even parity energy levels (cm^{-1}) of Mo V. New levels are noted with N.

Configuration	Term	J	Desig.[a]	Energy	Uncert.	Note	No. trans.
4p^{6}4d^2	^{3}F	2	d212	0.00	0.38		57
	^{3}F	3	d213	1577.17	0.39		75
	^{3}F	4	d214	3357.08	0.45		72
	^{1}D	2	d222	10 190.11	0.35		74
	^{3}P	0	d210	11 161.31	0.71		19
	^{3}P	1	d211	11 806.93	0.39		53
	^{3}P	2	d232	13 408.30	0.35		56
	^{1}G	4	d224	16 353.36	0.42		46
	^{1}S	0	d220	37 737.83	0.41		5
4p^{6}4d5s	^{3}D	1	sd11	92 380.54	0.09		16
	^{3}D	2	sd12	93 111.40	0.08		20
	^{3}D	3	sd13	94 835.44	0.09		15
	^{1}D	2	sd22	99 380.40	0.09		18
4p^{6}5s^2	^{1}S	0	s210	199 050.87	0.20	N	4
4p^{6}4d5d	^{1}F	3	5d13	232 561.12	0.06		17
	^{3}D	1	5d11	233 190.31	0.06		17
	^{3}D	2	5d12	234 252.45	0.06		19
	^{3}G	3	5d33	234 490.48	0.06		20
	^{3}G	4	5d14	235 496.01	0.08		13
	^{3}D	3	5d23	235 634.96	0.08		19
	^{1}P	1	5d21	236 002.02	0.08		13
	^{3}G	5	5d15	237 204.53	0.11		4
	^{3}F	2	5d22	237 759.53	0.08		15
	^{3}F	3	5d43	239 068.95	0.07		18
	^{3}S	1	5d31	239 188.82	0.08		15
	^{3}F	4	5d24	240 109.61	0.08		20
	^{1}D	2	5d32	241964.75	0.10		19
	^{3}P	0	5d10	242161.93	0.14		5
	^{3}P	1	5d41	242971.44	0.09		12
	^{3}P	2	5d42	243 954.32	0.09		16
	^{1}G	4	5d34	244 170.15	0.10		9
	^{1}S	0	5d20	251 017.96	0.32	N	3
4p^{6}4d6s	3/2[3/2]	1	6s11	254 125.95	0.03		12
	3/2[3/2]	2	6s12	254 464.98	0.03		16
	5/2[5/2]	3	6s13	256 676.48	0.03		13
	5/2[5/2]	2	6s22	257 442.81	0.03		14
4p^{6}5p^2	^{3}P	0	p210	314 344.75	0.29	N	2
	^{1}D	2	p212	320 344.53	0.28	N	5
	^{3}P	1	p211	320 917.27	0.24	N	4
	^{3}P	2	p222	323 777.46	0.23	N	4
	^{1}S	0	p220	349 643.4	1.8	N	1
4p^{6}4d5g	3/2[9/2]	5	5g15	327 070.61	0.26	N	4
	3/2[9/2]	4	5g14	327 141.68	0.29	N	3
	3/2[7/2]	3	5g13	327 386.30	0.76	N	1
	3/2[7/2]	4	5g24	327 436.40	0.27	N	3
	3/2[11/2]	5	5g25	327 859.16	0.34	N	2
	3/2[11/2]	6	5g16	327 995.37	0.24	N	3
	3/2[5/2]	3	5g23	328 234.03	0.38	N	2
	3/2[5/2]	2	5g12	328 265.06	0.28	N	4
	5/2[9/2]	5	5g35	329713.88	0.36	N	4
	5/2[9/2]	4	5g34	329 795.97	0.21	N	5
	5/2[11/2]	5	5g45	329 810.15	0.28	N	4
	5/2[11/2]	6	5g26	329 897.53	0.40	N	3
	5/2[7/2]	3	5g33	330 052.53	0.32	N	4
	5/2[7/2]	4	5g44	330 100.52	0.30	N	3
	5/2[13/2]	7	5g17	330 656.07	0.68	N	1
	5/2[5/2]	3	5g43	330 667.37	0.35	N	2
	5/2[5/2]	2	5g22	330 699.70	0.28	N	5
	5/2[13/2]	6	5g36	330 878.23	0.27	N	2

Table 2. (Continued.)

Configuration	Term	J	Desig.[a]	Energy	Uncert.	Note	No. trans.
	5/2[3/2]	1	5g11	331 233.74	0.38	N	1
	5/2[3/2]	2	5g32	331 263.46	0.23	N	4
$4p^6 5s5d$	^3D	1	ds11	346 764.00	0.60	N	1
	^3D	2	ds12	347 006.81	0.28	N	5
	^3D	3	ds13	347 408.70	0.39	N	3
	^1D	2	ds22	364 087.70[b]	0.76	N	2
$4p^6 5s6s$	^3S	1	ss11	368 808.38	0.48	N	3

[a] Designations are given with a short form of the configuration (two places) followed by the ordinal number of the calculated J value for the configuration (one place) and the J value (one place). For example, 5g36 indicates the third level with $J=6$ calculated for the 4d5g configuration.
[b] Not included in least-squares fit.

The 4d5d and 4d6s levels are plotted in figure 5. The 4d6s levels are designated in *jl*-coupling.

4.4. 4d4f + 4d6p levels

Nearly all of these levels were given in [6]. We have now located the missing 4d4f $^3H_6$ level from the newly found 4d4f–4d5g transition array. The 4d4f levels are plotted in figure 6. The 4d6p levels are plotted in figure 7.

Our 4d6p $^3P_0$ level at 280 279.0 cm^{-1} replaces the level in [6] at 280 451.5 cm^{-1}. The level in [6] was established by two lines: 372.235 Å, which was doubly classified, and 531.720 Å, which is expected to be too weak to be observed, and which is not present in our spectra. Our new 4d6p $^3P_0$ level makes six transitions to levels of $4d^2$, 4d5d, and 4d6s.

The position of the 4d4f $^3P_0$ level presented a special problem. Since the $4d^2$ ground configuration has only one level with $J=1$, 4d4f $^3P_0$ makes only one transition to $4d^2$. Cabeza *et al* [6] concluded that this transition was likely masked by the second order of an extremely strong line of Mo VII at 207.776 Å. This identification appeared to be confirmed by a weak transition to 4d5s $^3D_1$ at 624.671 Å. Unfortunately, the line at 624.671 Å does not appear in our spectra, although it is possibly masked by an extremely strong line of O IV at 624.617 Å. Nevertheless, careful examination of our spectra shows that the line at 415.530 Å is present at peak currents in the spark that are too low to excite Mo VII. We thus accept the identification of this line as the $4d^2$ $^3P_1$–4d4f $^3P_0$ transition, which confirms the 4d4f $^3P_0$ level given by Cabeza *et al* [6].

4.5. $5p^2$ + 5s5d levels

None of these levels were given in [6]. We have now located all five $5p^2$ levels based on their strong transitions to 4d5p and 5s5p. The $5p^2$ $^1S_0$ level is based on a single transition to 4d5p $^3D_1$ at 533.657 Å. Our calculations show that this configuration is strongly mixed with states of 4d6d, which has not yet been observed. In fact, the level at 320 917 cm^{-1}, which we designated $5p^2$ $^3P_1$, has dominant character of 4d6d $^3P_1$. Nevertheless, for simplicity we have retained the $5p^2$ $^3P_1$ designation for this level.

We also located all four of the possible 5s5d levels. They make transitions of moderate intensity to 5s5p. The 5s5d $^3D_1$ level is based on only a single transition to 5s5p $^3P_0$ at 998.556 Å. The 5s5d $^1D_2$ level deviates significantly from its calculated position and could not be included in the least-squares fits. As can be seen in table 5, this level (364 088 cm^{-1}) contains significant $5p^2$ $^1D_2$ character.

4.6. 5s4f levels

Three of the four possible levels of 5s4f were given by Tauheed *et al* [5]. We have now located the fourth $^3F_4$ by means of its transition to $4d^2$ $^3F_3$ at 288.936 Å. Although this transition would normally be prohibited as a two-electron jump, the admixture of other odd states allows the line to be observed. As in Zr III [7] and Nb IV [8], the 5s4f $^1F_3$ level is observed well below its predicted position; it is not included in our least-squares fit.

4.7. 4d5f levels

This group of levels is entirely new. As shown below, these levels are heavily mixed with levels of $4p^5 4d^3$ and their positions do not follow those of an unperturbed configuration. The levels are thus difficult to form into terms, and we omit a plot of the energy levels.

4.8. 4d5g levels

As mentioned earlier, locating these levels was the original purpose of this investigation. The process of finding these levels was complicated by the fact that most of the lines of the 4d4f–4d5g array fall in the region 1100–1200 Å. This is a difficult region for our observations, because the transmission of the MgF$_2$ window used to filter out the second order of diffraction drops rapidly here. The lowest wavelength observed with the MgF$_2$ window was 1138 Å. Exposures without the window were complicated by overlay of many second order lines. Nevertheless, we did find all 20 of the 4d5g levels.

Since 4d4f has levels with maximum J value of 6, the 4d5g 5/2[13/2]$_7$ level is necessarily based on only a single transition. The 4d4f $^3H_6$–4d5g 5/2[13/2]$_7$ transition is predicted to be the strongest line in this array, and we assign the

Table 3. Odd-parity energy levels (cm^{-1}) of Mo V. New levels are noted with N.

Configuration	Term	J	Desig.[a]	Energy	Uncert.	Note	No. trans.
4p^{6}4d5p	^{1}D	2	5p12	146 976.75	0.10		18
	^{3}D	1	5p11	148 948.66	0.10		17
	^{3}D	2	5p22	150 345.79	0.09		25
	^{3}F	3	5p13	151 195.14	0.09		23
	^{3}F	2	5p32	151 213.20	0.10		21
	^{3}D	3	5p23	153 039.67	0.11		21
	^{3}F	4	5p14	155 032.33	0.12		11
	^{3}P	1	5p21	156 616.49	0.10		19
	^{3}P	0	5p10	157 059.18	0.14		7
	^{3}P	2	5p42	157 851.46	0.11		20
	^{1}F	3	5p33	159 856.69	0.09		19
	^{1}P	1	5p31	162 257.12	0.09		18
4p^{6}5s5p	^{3}P	0	sp10	246 619.40	0.33		5
	^{3}P	1	sp11	247 932.56	0.27	was 4d4f	11
	^{3}P	2	sp12	254 209.83	0.19		10
	^{1}P	1	sp21	275 024.25	0.34	N	3
4p^{6}4d4f	^{1}G	4	4f14	237 482.33	0.24		8
	^{3}F	2	4f12	239 392.83	0.65		6
	^{3}H	4	4f24	239 949.69	0.25		7
	^{3}F	3	4f13	240 004.70	0.32		9
	^{3}H	5	4f15	240 725.04	0.29		6
	^{3}F	4	4f34	240 878.05	0.31		6
	^{1}D	2	4f22	241 752.33	0.26		11
	^{3}H	6	4f16	241 972.61	0.56	N	2
	^{3}G	3	4f23	243 408.59	0.29		7
	^{3}G	4	4f44	244 626.80	0.31		4
	^{3}G	5	4f25	245 600.22	0.40		3
	^{3}D	1	4f11	246 799.61	0.31	was 5s5p	8
	^{3}D	2	4f32	247 090.71	0.37		7
	^{3}D	3	4f33	247 687.61	0.28		7
	^{3}P	2	4f42	248 745.05	0.25		9
	^{1}F	3	4f43	250 990.91	0.26		6
	^{3}P	0	4f10	252 463.44	2.92		1
	^{3}P	1	4f21	252 648.40	0.21		11
	^{1}P	1	4f31	255 941.37	0.20		9
	^{1}H	5	4f35	259 254.51	0.19		5
4p^{6}4d6p	^{3}F	2	6p12	276 470.33	0.04		12
	^{3}D	1	6p11	277 187.91	0.04		11
	^{3}D	2	6p22	278 004.86	0.04		10
	^{3}F	3	6p13	278 999.30	0.04		10
	^{1}D	2	6p32	279 060.06	0.03		16
	^{3}D	3	6p23	279 478.11	0.05		15
	^{3}P	0	6p10	280 279.09	0.07	N	6
	^{3}P	1	6p21	280 505.47	0.05		8
	^{3}F	4	6p14	281 268.15	0.06		5
	^{1}F	3	6p33	281 996.44	0.04		11
	^{3}P	2	6p42	282 057.02	0.04		10
	^{1}P	1	6p31	285 619.22	0.07		10
4p^{6}4d5f	^{3}D	2	5f12	307 863.79	0.13	N	7
	^{3}D	1	5f11	310 475.83	0.21	N	3
	^{3}G	3	5f13	310 668.20	0.16	N	5
	^{3}H	4	5f14	311 070.16	0.17	N	6
	^{1}D	2	5f22	311 351.67	0.20	N	5
	^{3}G	5	5f15	311 959.68	0.27	N	3
	^{3}F	2	5f32	313 207.16	0.26	N	5
	^{3}F	3	5f23	313 772.78	0.92	N	1
	^{3}F	4	5f24	313 919.45	0.28	N	2
	^{3}H	4	5f34	314 526.51	0.16	N	4
	^{1}F	3	5f33	315 691.14	0.29	N	2

Table 3. (Continued.)

Configuration	Term	J	Desig.[a]	Energy	Uncert.	Note	No. trans.
	^{1}G	4	5f44	316 289.19	0.17	N	6
	^{3}H	5	5f25	316 463.94	0.18	N	4
	^{3}P	1	5f21	316 539.85	0.30	N	2
	^{3}H	6	5f16	316 643.63	0.33	N	1
	^{3}P	2	5f42	316 690.26	0.29	N	2
	^{1}H	5	5f35	319 648.03	0.23	N	4
	^{3}D	3	5f43	323 010.78	0.25	N	4
$4p^65s4f$	^{3}F	2	sf12	347 173.53	2.30		2
	^{3}F	3	sf13	347 303.47	2.24		3
	^{3}F	4	sf14	347 675	24	N	1
	^{1}F	3	sf23	351 932.60	2.91		2
$4p^64d6f$	^{3}G	5	6f15	349 517.6	5.5	N	2
	^{1}D	2	6f12	350 465.8	4.2	N	2
	^{3}F	2	6f22	351 332.7	4.4	N	2
	^{3}D	1	6f11	353 002.3	5.6	N	2
	^{1}F	3	6f13	353 268.9	2.4	N	4
	^{3}D	2	6f32	353 671.83	0.67	N	5
	^{3}F	3	6f23	354 169.92	0.71	N	5
	^{3}H	4	6f24	354 247.0	4.4	N	2
	^{3}H	5	6f25	354 542.54	0.50	N	3
	^{1}G	4	6f34	354 959.83	0.51	N	6
	^{3}P	0	6f10	355 095.6	5.9	N	1
	^{1}F	3	6f33	356 149.65	0.46	N	5
	^{1}H	5	6f35	356 387.52	0.73	N	2
	^{1}P	1	6f31	358 278.19	0.59	N	3
	^{3}G	3	6f43	363 720.6	4.7	N	2
	^{3}G	4	6f44	365 766.8	4.7	N	2
$4p^64d7f$	^{3}D	2	7f12	371 811.6	4.2	N	4
	^{1}H	5	7f15	372 444.9	4.9	N	2
	^{3}D	3	7f13	373 453.5	4.2	N	3
	^{3}F	2	7f32	375 034.5	3.8	N	5
	^{3}P	1	7f11	375 165.8	3.4	N	4
	^{3}F	3	7f23	375 355.1	4.1	N	3
	^{3}H	4	7f24	377 569.2	6.7	N	2
	^{1}G	4	7f34	377 999.3	4.0	N	3
	^{3}H	5	7f25	378 160.5	5.0	N	2
	^{3}G	3	7f43	381 105.4	5.0	N	2
	^{3}G	4	7f44	382 612.3	7.3	N	1
	^{3}G	5	7f35	383 279.5	5.0	N	2
	^{3}D	1	7f31	383 895.4	4.2	N	4
$4p^64d8f$	^{1}H	5	8f15	385 599.5	5.4	N	2
	^{1}D	2	8f12	386 020.8	6.2	N	4
	^{3}F	4	8f14	389 382.8	7.1	N	2
	^{1}F	3	8f13	389 461.4	4.6	N	3
	^{3}P	2	8f22	389 545.0	4.7	N	3
	^{1}G	4	8f34	392 544.3	4.6	N	3
	^{3}G	3	8f23	393 980.2	5.4	N	2
	^{3}D	1	8f21	394 631.2	7.4	N	2
	^{3}D	3	8f33	395 094.5	3.4	N	5
	^{3}D	2	8f42	395 126.4	5.4	N	3
	^{3}G	5	8f25	396 426.7	5.3	N	2
$4p^64d9f$	^{3}D	1	9f11	401 055.8	5.4	N	2
	^{3}H	4	9f14	401 751.2	5.7	N	2
	^{3}D	2	9f12	401 997.4	4.2	N	4
$4p^54d^3$		4	d14	280 277.2	3.9	N	1
		4	d24	287 427.8	3.1	N	2
		3	d23	287 471.4	4.1	N	1
		1	d21	287 818.7	4.2	N	1
		2	d32	287 997.7	4.1	N	1

Table 3. (Continued.)

Configuration	Term	J	Desig.[a]	Energy	Uncert.	Note	No. trans.
		2	d42	294 230.46	0.14	N	5
		5	d25	294 925.2	4.3	N	1
		4	d34	296 151.14	0.14	N	3
		3	d33	296 191.62	0.13	N	4
		3	d43	297 369.77	0.14	N	5
		2	d52	297 428.25	0.15	N	4
		4	d44	298 928.26	0.22	N	3
		1	d31	299 310.36	0.13	N	4
		3	d53	299 916.96	0.22	N	5
		5	d35	301 540.26	0.20	N	3
		4	d54	301 775.31	0.22	N	5
		0	d20	301 935.3	4.2	N	1
		2	d62	302 869.95	0.24	N	5
		1	d41	303 813.31	0.20	N	3
		3	d63	303 955.54	0.17	N	9
		3	d73	304 727.38	0.16	N	10
		6	d26	304 828.89	0.25	N	1
		2	d72	304 831.6	4.7	N	1
		4	d64	306 037.34	0.14	N	7
		5	d45	306 992.33	0.18	N	4
		4	d74	307 588.25	0.24	N	4
		3	d83	308 939.76	0.17	N	6
		3	d93	312 298.3	4.8	N	1
		2	d82	312 368.08	0.21	N	2
		5	d55	315 617.49	0.33	N	2
		3	d103	319 064.9	3.0	N	3
		0	d40	319 484.0	4.8	N	1
		2	d102	319 779.02	0.30	N	3
		3	d113	320 795.31	0.25	N	4
		4	d94	321 070.92	0.78	N	4
		1	d71	323 076.6	3.5	N	2
		4	d104	323 151.83	0.78	N	3
		3	d123	325 021.0	3.6	N	3
		2	d122	325 451.4	2.9	N	4
		4	d114	325 482.9	4.2	N	2
		5	d65	325 636.3	1.1	N	2
		2	d132	327 058.6	3.6	N	3
		0	d50	327 147.0	5.0	N	1
		2	d142	329 436.0	5.0	N	1
		4	d124	329 481.5	5.4	N	1
		5	d75	329 793.78	0.38	N	3
		3	d133	330 042.7	3.2	N	3
		5	d85	331 039.0	5.4	N	1
		1	d101	331 241.3	3.0	N	3
		4	d134	333 683.9	3.3	N	3
		3	d143	335 185.9	4.1	N	2
		0	d60	335 518.5	5.2	N	1
		2	d162	339 075.1	3.2	N	3
		3	d153	339 315.9	3.6	N	3
		5	d95	339 672.9	4.0	N	2
		2	d172	341 107.6	4.2	N	2
		4	d144	343 064.2	3.4	N	3
		3	d163	345 339.6	6.0	N	1
		4	d154	347 509.3	3.2	N	2
		3	d173	349 710.9	4.1	N	3
		4	d164	349 902.7	4.3	N	2
		2	d182	354 582.3	4.2	N	3
		3	d183	359 499.0	4.3	N	3
		2	d192	366 751.6	4.5	N	2

Table 3. (Continued.)

Configuration	Term	J	Desig.[a]	Energy	Uncert.	Note	No. trans.
		5	d105	366 892.6	4.6	N	2
		2	d202	367 517.4	4.5	N	2
		3	d193	368 492.2	4.6	N	2
		1	d141	371 078.1	3.7	N	4
		3	d203	384 886.5	4.2	N	4
		2	d212	385 431.2	3.4	N	5
		1	d151	386 919.8	3.3	N	5
		2	d222	387 095.3	4.7	N	3
		3	d213	388 410.0	4.0	N	4
		3	d223	397 682.6	4.4	N	3
		2	d242	398 182.6	4.4	N	3
		2	u01	387 420.8[b]	5.3	N	2
		3	u02	412 825.7[b]	5.9	N	2
		1	u03	414 658.8[b]	5.7	N	2

[a] For the two-electron type configurations, designations are given with a short form of the configuration (two places) followed by the ordinal number of the calculated J value for the configuration (one place) and the J value (one place). For example, 4f34 indicates the third level with $J = 4$ calculated for the $4d4f$ configuration. For the core-excited $4p^5 4d^3$ configuration, one place is used for the configuration short form (d), two places for the ordinal number, and one place for the J value. For example, d213 indicates the 21st level with $J = 3$ for the $4p^5 4d^3$ configuration.
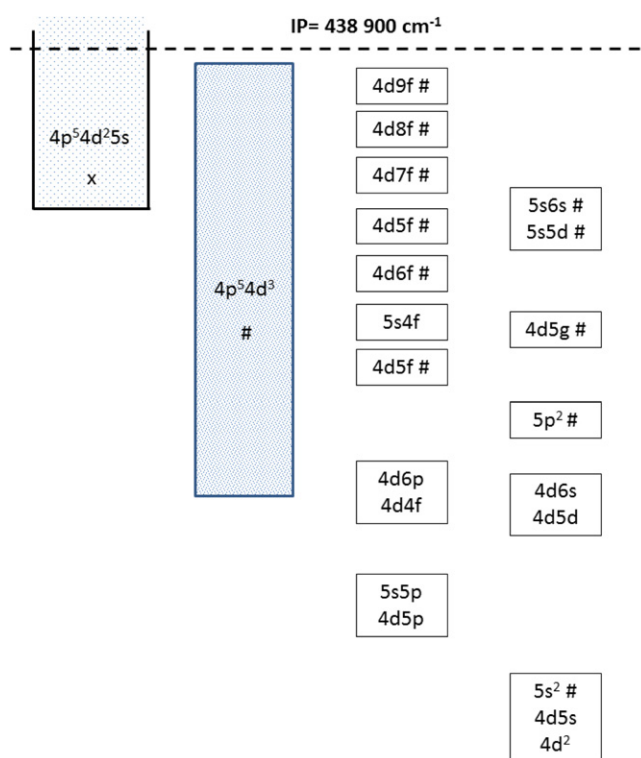[b] Unidentified level.

Figure 2. Schematic overview of the observed configurations for Mo V. Newly established configurations are noted by #. The $4p^5 4d^2 5s$ configuration, noted with an x, has no observed levels.

Figure 3. Structure of the $4d^2$, $4d5s$, and $5s^2$ configurations of Mo V. Levels of $4d5s$ are shown as dashed. The $5s^2\ ^1S_0$ level is shown as bold.

strong line at 1127.606 Å to this transition. This places 4d5g $5/2[13/2]_7$ close to its predicted position. There is little doubt about this assignment. On the other hand, we were not able to establish 4d5g $5/2[3/2]_1$ with certainty. The line that we use for our present identification is a weak line of Mo V character that places 4d5g $5/2[3/2]_1$ close to its expected position. The
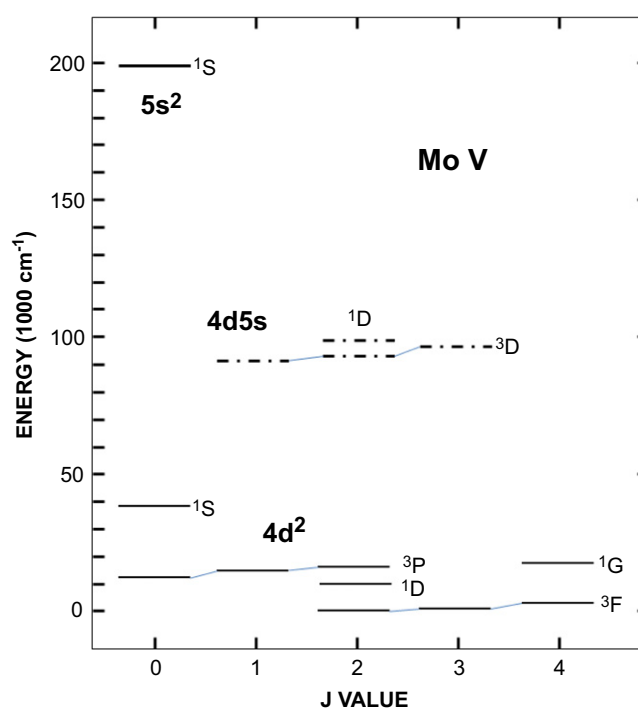
4d5g $3/2[7/2]_3$ level is also established by a single line, but this is a much stronger line and there is little doubt about the identification.

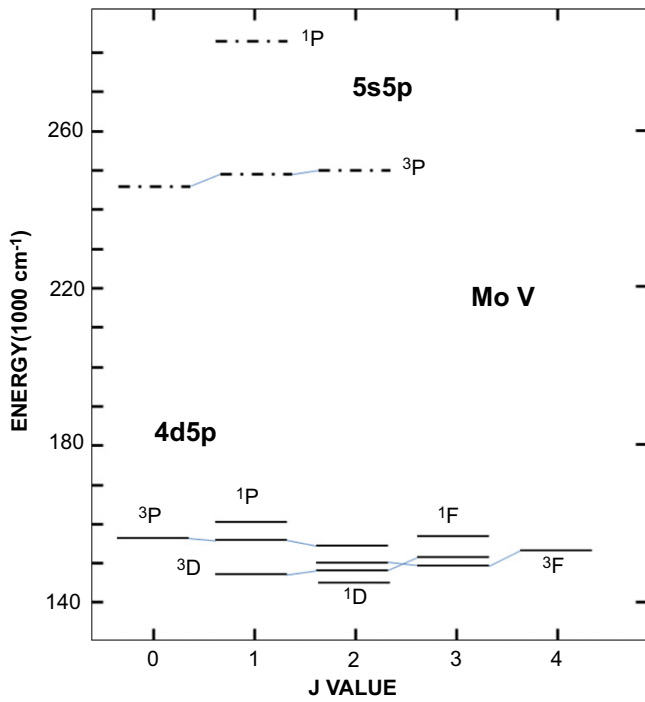The 4d5g levels are plotted in figure 8. The levels are designated in jl-coupling.

J. Phys. B: At. Mol. Opt. Phys. **48** (2015) 144001

J Reader and A Tauheed

Figure 4. Structure of the 4d5p and 5s5p configurations of Mo V. The 5s5p levels are shown as dashed.

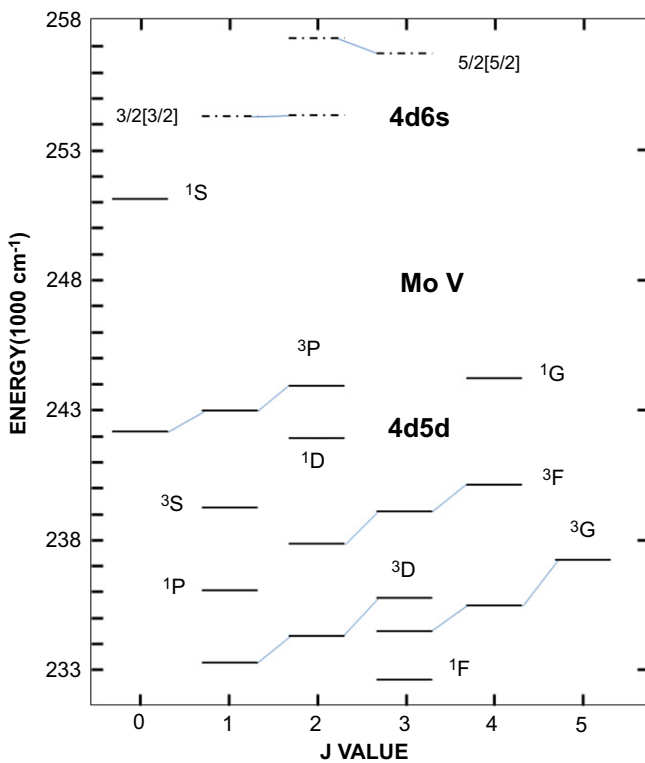**Figure 5.** Structure of the 4d5d and 4d6s configurations of Mo V. The 4d6s levels are shown as dashed and are designated in *jl*-coupling.

Figure 6. Structure of the 4d4f configuration of Mo V.

Figure 7. Structure of the 4d6p configuration of Mo V.

4.9. Higher 4dnf configurations

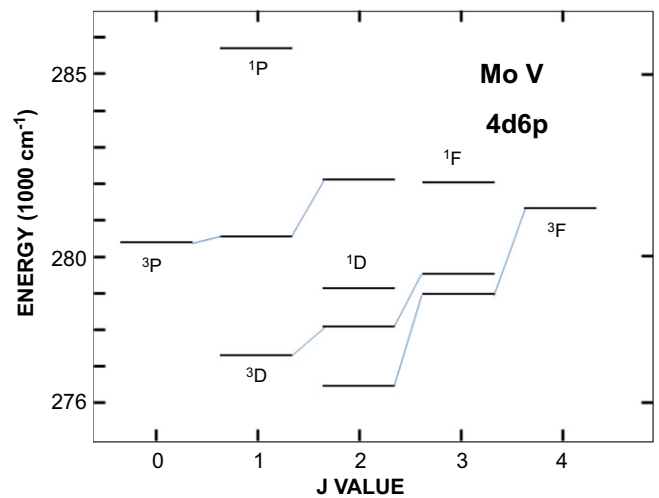Based on our calculations, we were able to locate a number of higher 4dnf ($n = 6, 7, 8, 9$) levels, although only the strongest transitions could be identified. For 4d9f only three levels were located. Nearly all of these levels are based on two or more transitions.

4.10. $4p^5 4d^3$ and $4p^5 4d^2 5s$ levels

Levels of the $4p^5 4d^3$ configuration make strong transitions to the ground $4p^6 4d^2$ configuration in the extreme vacuum ultraviolet. The $4p^5 4d^3$ configuration ranges from about $276\,000$ cm^{-1} to just below the ionization limit. This is shown schematically in figure 2. We have identified about 75 levels of this configuration. Many of these levels also make transitions to 4d5d levels. As can be seen from the last column in
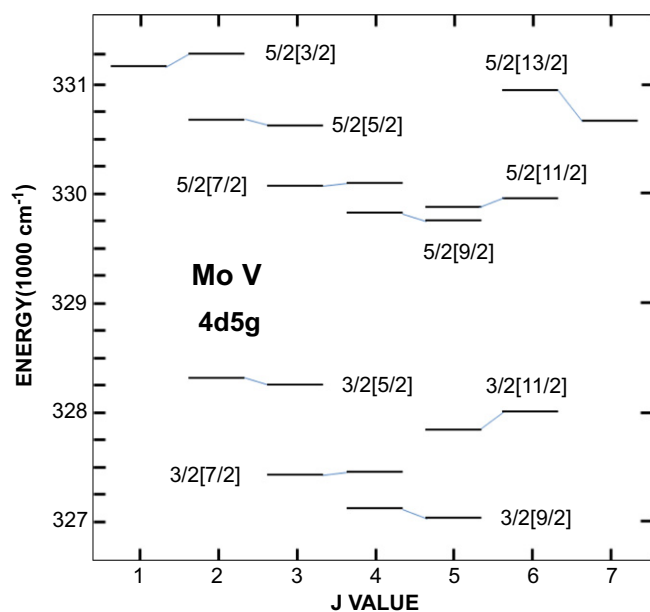
Figure 8. Structure of the 4d5g configuration of Mo V. The levels are designated in *jl*-coupling.

table 3, 16 of the $4p^54d^3$ levels are based on only a single line. However, these lines are definitely of Mo V character and place the level at its expected position.

As shown by the theoretical calculations, the $4p^54d^3$ levels are heavily mixed with levels of 4d5f and higher 4dnf configurations. This makes the naming of the levels ambiguous. In many cases our level labels have little physical meaning. Some levels labeled as $4p^54d^3$ actually have leading eigenvector components of 4d5f. As an example, the level of $4p^54d^3$ observed at 323 077 cm^{-1} (d71) has its three leading components as states of 4d5f. However, taking all of the components into account, the dominant character is in fact $4p^54d^3$.

As shown in figure 1 the $4p^54d^25s$ levels start very high in energy and range to well above the ionization limit. No experimental results are reported for them. A few levels in table 3 with no identifications (u01, u02, and u03) probably belong to this configuration.

5. Theoretical interpretation

5.1. Even configurations

The observed configurations were interpreted theoretically by making least-squares fits of the energy parameters to the observed levels with the Cowan suite of codes, RCN (Hartree–Fock code), RCG (energy matrix diagonalization code), and RCE (least-squares parameter fitting code) [13]. The Hartree–Fock code was run in a relativistic mode (HFR) with a correlation term in the potential. Breit energies were not included. For the initial calculations the HFR values were scaled by factors of 0.85 for the direct electrostatic parameters F^k and 0.80 for the exchange electrostatic parameters G^k and the CI parameters R^k. For the even levels the configurations

$4d^2 + 4d5s + 5s^2 + 4d5d + 4d6s + 5p^2 + 4d5g + 5s5d + 5s6s + 4d6d$ were treated as a single group. No configurations with open inner shells were included. The Hartree–Fock and least-squares fitted (LSF) parameters for the even configurations are given in table 4.

As shown, for the 5s5d configuration, the exchange interaction parameter $G^2(5s5d)$ was held fixed at a value that was slightly less than the HFR value. This was the same ratio as was used for this configuration in Nb IV [8]. The spin–orbit parameter ζ_{5d} was fixed at a value that was slightly higher than the HFR value. For the 5s6s configuration, where only the $^3S_1$ level was found, the exchange electrostatic parameter $G^0(5s6s)$ was fixed at its scaled HFR value. For the 4d5g configuration the exchange electrostatic parameters $G^2(4d5g)$, $G^4(4d5g)$, and $G^6(4d5g)$ were linked so as to maintain their HFR ratios.

The CI parameters that were allowed to vary were also linked at their HFR ratios. The remainder of the CI values were fixed at their scaled HFR values. They are not shown in table 4. The mean error of the fit of 30 free parameters to 65 levels of the even configurations was 97 cm^{-1}.

The calculated level values and the eigenvector compositions of the even configurations are given in table 5. (The complete table 5 is given in the supplementary materials.) As seen, there is not much mixing of configurations here. One exception is $5s^2$ $^1S_0$, which has 3% of $5p^2$ $^1S_0$ character. Another exception is for the $5p^2$ configuration, where the level designated as $5p^2$ $^3P_1$ (p211) has substantial 4d6d character; its leading percentage is actually 55% 4d6d $(^2D)^3P_1$. As in Zr III and Nb IV, the 4d5d $(^2D)^1G_4$ level deviates significantly from its calculated position. The deviations are: −169 cm^{-1} in Zr III [7], −220 cm^{-1} in Nb IV [8], and −351 cm^{-1} in Mo V. The reason for this deviation remains unknown. The 5s5d levels contain about 1% of 4d5g character.

5.2. Odd configurations

The odd configurations were treated together as the single group $4d5p + 4d6p + 5s5p + 5s6p + 5p5d + 5s4f + 4d4f + 4d5f + 4d6f + 4d7f + 4d8f + 4d9f + 4d10f + 4d11f + 4p^54d^3 + 4p^54d^25s$. No levels of the 5p5d, 4d10f, 4d11f or $4p^54d^25s$ configurations are known experimentally.

In table 6 we give the values of the parameters for the odd configurations. For this calculation, the values for ζ_{4d} for all the configurations were linked together so as to maintain their HFR ratios. The resulting ratio, 1.064, is reasonable. All values of ζ_{nf} were fixed at their HFR values. As seen, for many of the parameters the values were similarly linked. Parameters in each lettered group were linked together with their ratios fixed at the HFR values. The only CI parameters that were allowed to vary were those between the 4dnf configurations and $4p^54d^3$, and these were also linked at their HFR ratios. This was true for all of the CI parameters that were allowed to vary. The remainder of the CI parameters were fixed at their scaled HF values. They are not shown in table 6. All parameters for $4p^54d^3$ were allowed to vary freely. The fitted values are all well-defined and have

Table 4. Hartree–Fock (HFR) and least-squares fitted (LSF) parameters for the even configurations of Mo V. Mean error of fit: 97 cm^{-1}.

Configuration	Parameter	HFR[a]	LSF	Uncert.	Note[b]	LSF/HFR
$4p^64d^2$	$E_{av}(4p^64d^2)$	9081	8775	36		0.966
	$F^2(4d4d)$	67 314	55 099	220		0.819
	$F^4(4d4d)$	44 555	38 645	253		0.867
	ζ_{4d}	904	920	27		1.018
$4p^64d5s$	$E_{av}(4p^64d5s)$	96 673	95 274	50		0.988
	ζ_{4d}	969	984	52		1.015
	$G^2(4d5s)$	16 420	13 676	321		0.833
$4p^65s^2$	$E_{av}(4p^65s^2)$	205 610	203 515	171		0.991
$4p^64d5d$	$E_{av}(4p^64d5d)$	237 916	238 315	24		1.003
	ζ_{4d}	993	999	81		1.006
	ζ_{5d}	197	251	88		1.271
	$F^2(4d5d)$	18 395	15 584	207		0.847
	$F^4(4d5d)$	8848	7972	247		0.901
	$G^0(4d5d)$	5799	3868	38		0.667
	$G^2(4d5d)$	6375	5187	196		0.814
	$G^4(4d5d)$	5192	4191	238		0.807
$4p^64d6s$	$E_{av}(4p^64d6s)$	255 727	255 993	50		1.002
	ζ_{4d}	995	1021	44		1.026
	$G^2(4d6s)$	3738	2888	423		0.773
$4p^65s5d$	$E_{av}(4p^65s5d)$	349 870	348 287	57		0.996
	ζ_{5d}	218	229	(fixed)		1.052
	$G^2(5s5d)$	18 952	14214	(fixed)		0.750
$4p^64d5g$	$E_{av}(4p^64d5g)$	327 572	329 250	22		1.006
	ζ_{4d}	1005	1032	19		1.027
	ζ_{5g}	1	1	(fixed)		1.000
	$F^2(4d5g)$	6172	5165	211		0.837
	$F^4(4d5g)$	1853	1544	667		0.833
	$G^2(4d5g)$	1058	654	248	c	0.618
	$G^4(4d5g)$	700	432	164	c	
	$G^6(4d5g)$	515	318	121	c	
$4p^65s6s$	$E_{av}(4p^65s6s)$	368 965	370 209	97		1.004
	$G^0(5s6s)$	3637	2910	(fixed)		0.800
$4p^65p^2$	$E_{av}(4p^65p^2)$	324 214	323 741	79		0.999
	$F^2(5p5p)$	39 643	36471	564		0.920
	ζ_{5p}	2517	3056	83		1.214
Configuration interaction						
$4p^64d^2$–$4p^64d5s$	$R^2(4d4d,4d5s)$	−16 841	−14 263	237	d	0.847
$4p^64d^2$–$4p^65s^2$	$R^2(4d4d,5s5s)$	18 980	16 074	267	d	
$4p^64d^2$–$4p^65p^2$	$R^1(4d4d,5p5p)$	13 422	11 367	189	d	
	$R^3(4d4d,5p5p)$	11 804	9997	166	d	
$4p^64d5s$–$4p^65p^2$	$R^1(4d5s,5p5p)$	−19 670	−16 659	277	d	
$4p^65s^2$–$4p^65p^2$	$R^1(5s5s,5p5p)$	50953	43 152	716	d	
$4p^64d5d$–$4p^65p^2$	$R^1(4d5d,5p5p)$	−12 691	−10 748	178	d	
	$R^3(4d5d,5p5p)$	−8006	−6781	113	d	
$4p^64d6s$–$4p^65p^2$	$R^1(4d6s,5p5p)$	−160	−135	2	d	
$4p^64d5g$–$4p^65p^2$	$R^3(4d5g, 5p5p)$	−5651	−4786	79	d	
$4p^65s6s$–$4p^65p^2$	$R^1(5s6s,5p5p)$	−1698	−1438	24	d	
$4p^65p^2$–$4p^64d6d$	$R^1(5p5p,4d6d)$	−5995	−5077	84	d	
	$R^3(5p5p,4d6d)$	−4529	−3836	64	d	

[a] HFR values of average values of configurations adjusted so that energy of $4p^64d^2$ $^3F_2 = 0$ cm^{-1}.
[b] c, d: linked in LSF.

reasonable HFR ratios. This provides a measure of support for our interpretation of these levels. The mean error of the fit of 32 free parameters to 188 levels of the odd configurations was 358 cm^{-1}.

The calculated level values and the eigenvector compositions for the odd configurations are given in table 7. (The complete table 7 is given in the supplementary materials.) Included in this table are calculated level values and compositions for a few levels that were not observed. We note that not all possible levels of $4p^54d^3$ are covered by the levels in table 7. This is caused by the distribution of $4p^54d^3$ character throughout the system of odd levels to the extent that some

Table 5. Calculated energy levels (cm^{-1}) and percentage compositions for the even configurations of Mo V. Complete table is given in supplementary materials.

J	Obs.	Calc.	O−C	% $j\ell$		Percentage composition (LS)								
2	0	−60	60			98%	4d^2	(^{3}F)^{3}F	2%	4d^2	(^{1}D)^{1}D			
2	331 263	331 259	4	98%	5/2[3/2]	54%	4d5g	(^{2}D) ^{3}D	45%	4d5g	(^{2}D) ^{1}D	1%	5s5d	(^{2}s) ^{3}D
1	346 764	346 802	−38			99%	5s5d	(^{2}S) ^{3}D	1%	4d5g	(^{2}D) ^{3}D			
2	347 007	347 018	−11			99%	5s5d	(^{2}S) ^{3}D	1%	4d5g	(^{2}D) ^{3}D			
3	347 409	347 353	56			99%	5s5d	(^{2}S) ^{3}D	1%	4d5g	(^{2}D) ^{3}D			
2	364 088[a]	362 074				77%	5s5d	(^{2}S) ^{1}D	21%	5p^2	(^{1}D) ^{1}D	1%	4d5g	(^{2}D) ^{1}D
1	368 808	368 808	0			100%	5s6s	(^{2}S) ^{3}S						
0		374 723				100%	5s6s	(^{2}S) ^{1}S						

[a] Not included in least-squares fit.

levels appear to be missing. For example, for 4p^{5}4d^3 in table 7, there are 17 levels having $J=1$, although 19 are possible. This is a consequence of our attempt to group the levels by configuration. The complete eigenvectors, which we do not present, reflect all the components accurately.

As already discussed, the 4dnf levels contain large admixtures of 4p^{5}4d^3 and 5s5p. As shown in table 7, the 5s5p levels contain large admixtures of 4d4f and 4d6p character.

6. Oscillator strengths

The wave functions obtained with the fitted values of the energy parameters were used to calculate weighted oscillator strengths gf and weighted transition probabilities gA for all classified lines. The values of log gf, f being the oscillator strength and g the statistical weight of the lower level $2J_L+1$, are given in table 1. The values of gA, A being the transition probability and g the statistical weight of the upper level $2J_U+1$, are also given in this table.

7. Comparison with *ab initio* theory

Pan and Beck [15] used their Relativistic CI method to calculate energy levels and transition probabilities for the 9 lowest $J=0$ levels of even parity and the 30 lowest $J=1$ levels of odd parity of Mo V. They compared their level values for the normal valence configurations with the experimental values and found agreement to about 200 cm^{-1}. Since levels of 4p^{5}4d^3 were not known at the time, comparison of their calculated levels for this configuration was not possible. Now that we have located quite a few 4p^{5}4d^3 levels experimentally, a comparison can be made. Unfortunately, we are not able to correlate their values and our present ones. This may be due to omission of 4dnf ($n>4$) configurations in their calculations.

In table 8 we compare Pan and Beck's calculated f-values with our present values. For transitions in which the $J=1$ level is lower than the $J=0$ level, we have reduced their f-values by a factor of 3, as called for in their table IV. Considering the complexity of the spectrum, the f-values agree reasonably well, usually within about 20%.

8. Ionization energy

Cabeza *et al* [6] derived a value for the ionization energy of Mo V from the two member series 4dns($n=5$, 6) and the two member series 4dnp($n=5$, 6) with values of Δn^* taken from the one-electron spectrum Nb V [17]. With a value of Δn^* for the 4dns series taken as 1.035 and for the 4dnp series as 1.033, they obtained values for the ionization energy of 439 326 ± 250 and 439 606 ± 250 cm^{-1}, respectively, and adopted an average value of 439 450 ± 200 cm^{-1}. No explanation for the individual uncertainties of ±250 cm^{-1} was given.

For our present determination, we use the Cowan code to calculate the term value T of the 4d5g configuration. For this calculation we subtract the binding energy given by the code for the 4d5g configuration of Mo V from that of the 4p^6 ground configuration of Mo VI. This yields T(4d5g)$=$ 111 212 cm^{-1}. To estimate an uncertainty for this value, we compare term values for the 5g configuration calculated with the Cowan code with values observed for Rb-like spectra. Since the term values have been accurately determined from experiment for these spectra, we can use them to estimate the accuracy of the calculated term values. The results are shown in table 9. For the calculated term values the uncertainty is taken as one unit in the last decimal place for the binding energy, 1 cm^{-1}. From this comparison, we conclude that the calculated term value is accurate to a few tens of cm^{-1}, and we estimate the uncertainty of the calculated term value for Mo V as ±150 cm^{-1}.

With a center-of-gravity for the 4d5g configuration calculated from the observed levels in table 2 (329 235.3 cm^{-1}) we obtain a limit of 440 447 ± 150 cm^{-1}. Reducing this by the average energy of the 4d configuration of Mo VI [10], 1550.1 cm^{-1}, we find the ionization energy of Mo V to be 438 897 ± 150 cm^{-1}. Rounding to the nearest 10 cm^{-1}, we have for our final value of the ionization energy 438 900 ± 150 cm^{-1} (54.417 ± 0.019 eV) [18].

This value can be compared with the *ab initio* calculated value 53 eV published by Rodrigues *et al* [19]. This follows the trend for the comparison of the values from [19] relative to observed values recently pointed out by Reader *et al* [20].

Table 6. Hartree–Fock (HFR) and least-squares fitted (LSF) parameters for the odd configurations of Mo V. Mean error of fit: 358 cm^{-1}.

Configuration	Parameter	HFR	LSF	Uncert.	Note[a]	LSF/HFR
$4p^6 4d5p$	$E_{av}(4p^6 4d5p)$	154 494	155 581	108		1.010
	ζ_{4d}	978	1041	51	a	1.064
	ζ_{5p}	2293	2780	252		1.212
	$F^2(4d5p)$	28 490	23 641	992		0.830
	$G^1(4d5p)$	10 645	9601	533		0.902
	$G^3(4d5p)$	9694	7861	947		0.811
$4p^6 5s5p$	$E_{av}(4p^6 5s5p)$	257417	258 141	312		1.004
	ζ_{5p}	2552	3370	409		1.320
	$G^1(5s5p)$	50 892	38 336	1201		0.753
$4p^6 4d6p$	$E_{av}(4p^6 4d6p)$	279 660	280 363	111		1.004
	ζ_{4d}	997	1061	52	a	1.064
	ζ_{6p}	965	1141	317		1.183
	$F^2(4d6p)$	10 581	8870	1115		0.838
	$G^1(4d6p)$	2875	2370	523	b	0.824
	$G^3(4d6p)$	2959	2440	539	b	0.824
$4p^6 4d4f$	$E_{av}(4p^6 4d4f)$	249 088	249 095	125		1.001
	ζ_{4d}	980	1043	51	a	1.064
	ζ_{4f}	7	7		c	1.000
	$F^2(4d4f)$	30 965	27 857	719	d	0.900
	$F^4(4d4f)$	17 573	15 837	409	d	
	$G^1(4d4f)$	30 844	25 446	365	e	0.825
	$G^3(4d4f)$	18 416	15 194	218	e	
	$G^5(4d4f)$	12 790	10 552	151	e	
$4p^6 4d5f$	$E_{av}(4p^6 4d5f)$	318 014	318 040	158		1.001
	ζ_{4d}	994	1058	52	a	1.064
	ζ_{5f}	5	5		c	1.000
	$F^2(4d5f)$	13 750	12 369	319	d	0.900
	$F^4(4d5f)$	7756	6977	180	d	
	$G^1(4d5f)$	13 657	11 267	162	e	0.825
	$G^3(4d5f)$	8568	7068	101	e	
	$G^5(4d5f)$	6068	5004	72	e	
$4p^6 4d6f$	$E_{av}(4p^6 4d6f)$	355 752	356 192	133		1.002
	ζ_{4d}	1000	1064	52	a	1.064
	ζ_{6f}	3	3		c	1.000
	$F^2(4d6f)$	7166	6447	166	d	0.900
	$F^4(4d6f)$	4042	3636	94	d	
	$G^1(4d6f)$	6886	5681	82	e	0.825
	$G^3(4d6f)$	4437	3660	53	e	
	$G^5(4d6f)$	3177	2621	38	e	
$4p^6 4d7f$	$E_{av}(4p^6 4d7f)$	378 358	378 961	152		1.002
	ζ_{4d}	1002	1067	52	a	1.064
	ζ_{7f}	2	2		c	1.000
	$F^2(4d7f)$	4212	3790	98	d	0.900
	$F^4(4d7f)$	2379	2141	55	d	
	$G^1(4d7f)$	3945	3254	47	e	0.825
	$G^3(4d7f)$	2584	2132	31	e	
	$G^5(4d7f)$	1862	1537	22	e	
$4p^6 4d8f$	$E_{av}(4p^6 4d8f)$	392 887	393 797	202		1.003
	ζ_{4d}	1004	1068	52	a	1.064
	ζ_{8f}	1	1		c	1.000
	$F^2(4d8f)$	2691	2421	62	d	0.900
	$F^4(4d8f)$	1522	1369	35	d	
	$G^1(4d8f)$	2474	2041	29	e	0.825
	$G^3(4d8f)$	1638	1351	19	e	
	$G^5(4d8f)$	1186	978	14	e	
$4p^6 4d9f$	$E_{av}(4p^6 4d9f)$	402 764	403 453	329		1.003
	ζ_{4d}	1005	1069	52	a	1.064
	ζ_{9f}	1	1		c	0.900
	$F^2(4d9f)$	1826	1552		c	0.850

Table 6. (Continued.)

Configuration	Parameter	HFR	LSF	Uncert.	Note[a]	LSF/HFR
	F^4(4d9f)	1034	879		c	0.850
	G^1(4d9f)	1657	1326		c	0.800
	G^3(4d9f)	1105	884		c	0.800
	G^5(4d9f)	803	642		c	0.800
$4p^64f5s$	$E_{av}(4p^64f5s)$	357 870	355417	243		0.994
	ζ_{4f}	10	10		c	1.000
	G^3(4f5s)	28 497	22 809	2546		0.800
$4p^54d^3$	$E_{av}(4p^54d^3)$	333 311	328 490	84		0.986
	F^2(4d4d)	67 962	52 849	501		0.778
	F^4(4d4d)	45 011	36 942	698		0.821
	ζ_{4p}	13 361	13 787	174		1.032
	ζ_{4d}	929	821	69		0.883
	F^2(4p4d)	73 491	65 479	537		0.891
	G^1(4p4d)	91 867	68 487	373		0.746
	G^3(4p4d)	56 652	48 743	821		0.860
$4p^54d^25s$	$E_{av}(4p^54d^25s)$	423 100	423 100	(fixed)	c	1.000
	F^2(4d4d)	70 038	59 532	(fixed)	c	0.850
	F^4(4d4d)	46 528	39 549	(fixed)	c	0.850
	ζ_{4p}	13 720	13 720	(fixed)	c	1.000
	ζ_{4d}	994	994	(fixed)	c	1.000
	F^2(4p4d)	75 472	64 151	(fixed)	c	0.850
	G^1(4p4d)	94 553	75 642	(fixed)	c	0.800
	G^3(4p4d)	58 466	46 773	(fixed)	c	0.800
	G^1(4p5s)	8075	6460	(fixed)	c	0.800
	G^2(4d5s)	16 381	13 104	(fixed)	c	0.800
Configuration interaction						
$4p^64d4f$–$4p^54d^3$	R^1(4p4f,4d4d)	48 456	36 388	401	f	0.751
	R^3(4p4f,4d4d)	27 515	20663	227	f	
$4p^64d5f$–$4p^54d^3$	R^1(4p5f,4d4d)	33 532	25 181	277	f	
	R^3(4p5f, 4d4d)	20 182	15 156	167	f	
$4p^64d6f$–$4p^54d^3$	R^1(4p6f, 4d4d)	24 021	18 039	199	f	
	R^3(4p6f, 4d4d)	14 838	11 143	123	f	
$4p^64d7f$–$4p^54d^3$	R^1(4p7f, 4d4d)	18 223	13 685	151	f	
	R^3(4p7f,4d4d)	11 416	8573	94	f	
$4p^64d8f$–$4p^54d^3$	R^1(4p8f,4d4d)	14 439	10 843	119	f	
	R^3(4p8f, 4d4d)	9122	6850	75	f	

[a] a, b, d, e, f- linked in groups in LSF; c—fixed at scaled HFR value.

Table 7. Calculated energy levels (cm^{-1}) and percentage compositions for the odd configurations of Mo V. Integers following the final term symbols represent the seniority of the parent term of the 4d^3 configuration. Lower case letters following the final term symbol represent the seniority of the parent term of the 4d^{2}5s configuration. Complete table is given in supplementary materials.

J	Obs.	Calc.	O − C	%$j\ell$	Percentage composition (LS)								
2	146 977	147 031	−54		55%	4d5p	$(^2D)^1D$	40%	4d5p	$(^2D)^3F$	3%	4d5p	$(^2D)^3D$
1	148 949	148 827	122		93%	4d5p	$(^2D)^3D$	4%	4d5p	$(^2D)^1P$	2%	4d5p	$(^2D)^3P$
2	398 183	398 574	−391		26%	4d8f	$(^2D)^3P$	20%	4d8f	$(^2D)^1D$	15%	4d9f	$(^2D)^3P$
1		408 005			21%	4d9f	$(^2D)^1P$	19%	p^{5}d^3	$(^2P)^1P$	19%	4d10f	$(^2D)^1P$
3		408 278			20%	p^{5}d^3	$(^2F)^1F$	15%	p^{5}d^3	$(^2D)^1F2$	14%	p^{5}d^3	$(^2G)^1F$
1		428 757			40%	p^{5}d^3	$(^2D)^1P1$	33%	5p5d	$(^2P)^1P$	7%	4d11f	$(^2D)^1P$

9. Summary

We observed the spectrum of Mo V from 200 to 4700 Å with sliding spark discharges and diffraction grating spectrographs and identified about 600 new lines and 130 new energy levels.

The levels were interpreted theoretically by means of Hartree–Fock calculations and least-squares fitting of the energy parameters to the observed levels. The fitted parameters were used to calculate oscillator strengths for all classified lines. Accurate Ritz-type wavelengths were determined for a large

J. Phys. B: At. Mol. Opt. Phys. **48** (2015) 144001

J Reader and A Tauheed

Table 8. Comparison of *f*-values of Pan and Beck [13] with present values.

Transition		Wavelength(Å)[a]	Pan and Beck		*f* (present)	Intensity[b]	
J = 0	*J* = 1		Length	Velocity			
4d² ³P	4d5p ³D	725.759	0.094	0.093	0.107	3000	dc
	4d5p ³P	687.497	0.163	0.161	0.186	2000	
	4d5p ¹P	661.830	0.024	0.023	0.033	75	
	5s5p ³P	422.353	0.117	0.123	0.047	100	
	4d4f ³D	424.382	0.564	0.590	0.768	350	
	4d4f ³P	414.106	0.107	0.111	0.132	75	
	4d6p ³D	375.905	0.010	0.010	0.010	5	
	4d6p ³P	371.273	0.022	0.023	0.024	25	
4d² ¹S	4d5p ³P	841.196	0.013	0.013	0.018	300	
	4d5p ¹P	803.087	0.218	0.211	0.247	600	
	4d4f ¹P	458.291	0.812	0.843	1.038	350	
	4d6p ¹P	403.416	0.098	0.102	0.101	60	
5S² ¹S	4d4f ¹P	1757.764	0.294	0.294	0.247	200	
	5s5p ¹P	1613.250	1.060	1.080	1.280	400	
	4d6p ³D	1279.790	0.112	0.118	0.270	50	dc
	4d6p ¹P	1155.156	0.314	0.322	0.432	400	
4d5d ³P	4d5p ³D	1072.806	0.069	0.070	0.088	700	
	4d5p ³P	1168.969	0.123	0.124	0.140	2500	
	4d5p ¹P	1251.489	0.009	0.009	0.012	1	
4d5d ¹S	4d5p ³P	1059.302	0.004	0.004	0.007	20	
	4d5p ¹P	1126.624	0.171	0.170	0.192	2000	
5p² ³P	4d5p ³D	604.604	0.104	0.112	0.092	5	
	4d4f ³P	1620.842	0.039	0.037	0.074	2	
5p² ¹S	4d5p ¹P	533.657	0.148	0.149	0.187	35	

[a] Observed wavelength in vacuum.
[b] Intensity observed in present work; dc, doubly classified line.

Table 9. Observed and calculated 5g term values (cm⁻¹) for Rb-like ions. Observed values taken from NIST atomic spectra database [21].

Spectrum	*T*(obs.)	*T*(calc.)	Obs. − calc.
Rb I	4394.61 ± 0.01	4393 ± 1	2 ± 1
Sr II	17 607.4 ± 0.1	17 600 ± 1	7 ± 1
Y III	39 704.3 ± 1.0	39 716 ± 1	−12 ± 2
Zr IV	70 738.2 ± 0.5	70 793 ± 1	−55 ± 1
Nb V	110 803 ± 40	110 847 ± 1	−44 ± 40

number of lines in the vacuum ultraviolet. An improved value for the ionization energy was determined from the 4d5g configuration.

Acknowledgments

References

[1] Churilov S S and Ryabtsev A N 2006 *Opt. Spectrosc.* **101** 169
Churilov S S and Ryabtsev A N 2006 *Opt. Spectrosk.* **101** 181 (Russian)
[2] Kučas S, Karazija R, Jonauskas V and Momkauskaitė A 2009 *J. Phys. B: At. Mol. Opt. Phys.* **42** 205001
[3] Trawick M W 1935 *Phys. Rev.* **48** 223
[4] Moore C E 1952 *Atomic Energy Levels as Derived From the Analyses of Optical Spectra* vol II NBS Circular 467 (Washington, DC: US Government Printing Office)
[5] Tauheed A, Chaghtai M S Z and Rahimullah K 1985 *Phys. Scr.* **31** 369
[6] Cabeza M I, Meijer F G and Iglesias L 1986 *Phys. Scr.* **34** 223
[7] Reader J and Acquista N 1997 *Phys. Scr.* **55** 310
[8] Tauheed A and Reader J 2005 *Phys. Scr.* **72** 158
[9] Reader J, Epstein G L and Ekberg J O 1972 *J. Opt. Soc. Am.* **62** 273
[10] Reader J 2010 *J. Phys. B: At. Mol. Opt. Phys.* **43** 074024
[11] Reader J and Feldman U 1990 *J. Opt. Soc. Am.* B **7** 253
[12] The program ELCALC was written by L J Radziemski Jr (The Research Corporation, Tuscon, Arizona, 85712, USA). The procedure and definition of level value uncertainties are described by Radziemski L J, Jr and Kaufman V 1969 *J. Opt. Soc. Am.* **59** 424
[13] Cowan R D 1981 *The Theory of Atomic Structure and Spectra* (Berkeley, CA: University of California Press) and Cowan programs RCN, RCN2, RCG, and RCE
[14] Reader J 1997 *Comp. Phys.* **11** 190
[15] Pan L and Beck D R 2004 *Phys. Scr.* **70** 257
[16] Beck D R and Pan L 2004 *Phys. Scr.* **69** 91
[17] Kagan D T, Conway J G and Meinders E 1981 *J. Opt. Soc. Am.* **71** 1193

[18] Conversion of the ionization energy from cm^{-1} to eV was done with the factor 8065.544 29(18) cm^{-1} eV^{-1} given by Mohr P J, Taylor B N and Newell D B 2012 *Rev. Mod. Phys.* **84** 1527

[19] Rodrigues G C, Indelicato P, Santos J P, Patté P and Parente F 2004 *At. Data Nucl. Data Tables* **86** 117

[20] Reader J, Gillaspy J D, Osin D and Yu Ralchenko 2014 *J. Phys. B: At. Mol. Opt. Phys.* **47** 145003

[21] Kramida A, Ralchenko Yu, Reader J and Team NIST ASD 2013 *NIST Atomic Spectra Database* (version 5.1). Available: (http://physics.nist.gov/asd)